Magnetic Resonance Imaging of Inflammation With a Specific Selectin-Targeted Contrast Agent

Sébastien Boutry,[1] Carmen Burtea,[1] Sophie Laurent,[1] Gérard Toubeau,[2] Luce Vander Elst,[1] and Robert N. Muller[1]*

E-selectin-targeted contrast enhancement of blood vessels in inflamed tissues was investigated with a new contrast agent, Gd-DTPA-B(sLe^x)A, which was recently obtained by grafting a synthetic mimetic of sialyl-Lewis^x, an E-selectin ligand, onto Gd-DTPA. The pharmacokinetics, biodistribution, and potential to image inflammation by MRI of this E-selectin-targeted contrast agent were evaluated. The inhibition (by 15–34%) produced by Gd-DTPA-B(sLe^x)A on Sialyl Le^x-PAA-biotin binding to E-selectin confirmed the specific interaction of the new contrast agent with this adhesion molecule. Gd-DTPA-B(sLe^x)A was tested at a dose of 0.1 mmol/kg b.w. on mice and rats in a fulminant hepatitis model induced by the co-administration of D-galactosamine and *E. coli* lipopolysaccharide. A significant and prolonged contrast enhancement between blood vessels and liver parenchyma was obtained in pathological conditions, which attests to the specificity of the agent for E-selectin. The prolonged vascular residence (48.9 min in hepatitis vs. 29.8 min in healthy animals), as evidenced by the pharmacokinetic characterization, suggests that Gd-DTPA-B(sLe^x)A interacts with the specific receptors expressed during inflammation. The biodistribution of the compound indicates its retention in inflamed liver by both specific mechanisms and nonspecific accumulation due to the necrotic lesions. The same mechanisms are invoked to account for its retention in the spleen. Magn Reson Med 53:800–807, 2005. © 2005 Wiley-Liss, Inc.

Key words: inflammation; E-selectin; sialyl-Lewis^x; adhesion molecules; MRI

Inflammation is defined as the reaction of the body to any kind of injury (1,2). It involves the activation of powerful defense mechanisms involving cells (leukocytes) and plasma proteins (opsonins, antibodies, and complement) that converge on the injury site. Vasoactive and chemotactic mediators generated at the inflammation site are responsible for this recruitment. The subsequent extravasation is facilitated by vasodilatation and increased endothelial permeability in conjunction with the expression of adhesion molecules on endothelial cells and leukocytes. The leukocytes' rolling, arrest, and adhesion on the vascular endothelium, as well as their diapedesis through the endothelium and the basal membrane, are mediated by specific adhesion molecules, such as integrins, selectins, and the superfamily of immunoglobulins (3–5).

The in vivo detection of inflammation provides a valuable tool for diagnosing a broad range of pathologies with an inflammatory profile (i.e., infection, neoplasm, atherosclerosis, ischemia, etc.), and for monitoring their therapy. On the other hand, the changes in a tissue's biochemistry that occur during inflammation offer suitable targets for tracers that could facilitate the imaging of inflammatory foci in the early phases, before the anatomical changes become evident (1,6).

Several approaches have been developed over the past 30 years to visualize inflammation/infection with the use of specific radiopharmaceuticals. Among the strategies considered by nuclear medicine, one can mention the targeting of leukocytes or mediators moving to or present at the site of inflammation/infection, and the confirmation of an increased glucose uptake by infiltrated granulocytes and tissue macrophages (1).

Contrast-enhanced MR imaging (CE-MRI) has greatly improved our understanding of the pathophysiology of inflammatory diseases, such as multiple sclerosis (7), inflammatory myopathies (8), rheumatoid arthritis (9), and endocarditis (10). However, a modest correlation between the image enhancement and the evolution of the inflammatory lesion is sometimes encountered. This has been attributed to the limited sensitivity and specificity of MRI carried out with nonspecific agents (7). MRI is nevertheless a pertinent technique for temporal studies, and is advantageous because it can simultaneously sample large regions of interest (ROIs). Direct targeting of MR contrast agents to receptors within the pathological region has the obvious potential of achieving greater specificity than "passive" targeting approaches.

In the present study we developed a molecular imaging strategy to target E-selectin with a mimetic of its ligand, the sialyl-Lewis^x (Fig. 1). Members of the selectin family (L-, E-, and P-selectin) have all been shown to be capable of mediating neutrophil rolling in vitro and in vivo (11). E-selectin is a membrane glycoprotein that is transiently expressed on the endothelial cells after stimulation with TNF-α, IL-1, and bacterial lipopolysaccharide (12–14). MRI of E-selectin expression in human endothelial cell cultures was recently assessed with cross-linked iron oxide nanoparticles (CLIO) functionalized with anti-human E-selectin antibodies (15).

A mimetic molecule reported in the literature (16) preserves its affinity for E-selectin because of the conformation of 2-(α-D-mannopyranosyloxy)-biphenyl, which maintains some of the structure features of sialyl-Lewis^x through the simultaneous presence of the hydroxyl groups on mannose and the carboxylate function on a phenyl

[1]Department of Organic and Biomedical Chemistry, NMR and Molecular Imaging Laboratory, Mons, Belgium.

[2]Laboratory of Histology and Experimental Cytology, University of Mons-Hainaut, Mons, Belgium.

Grant sponsor: French Community of Belgium, ARC Program; Grant numbers: 95/00-194; 00-05/258.

Presented in part at the 9th Annual Meeting of ISMRM and the 8th Annual Meeting of ESMRMB, Glasgow, Scotland, 2001.

*Correspondence to: Professor Robert N. Muller, Department of Organic and Biomedical Chemistry, University of Mons-Hainaut, 24, Avenue du Champ de Mars, B-7000 Mons, Belgium. E-mail: Robert.Muller@umh.ac.be

Received 20 July 2004; revised 22 October 2004; accepted 22 October 2004.

DOI 10.1002/mrm.20403

Published online in Wiley InterScience (www.interscience.wiley.com).

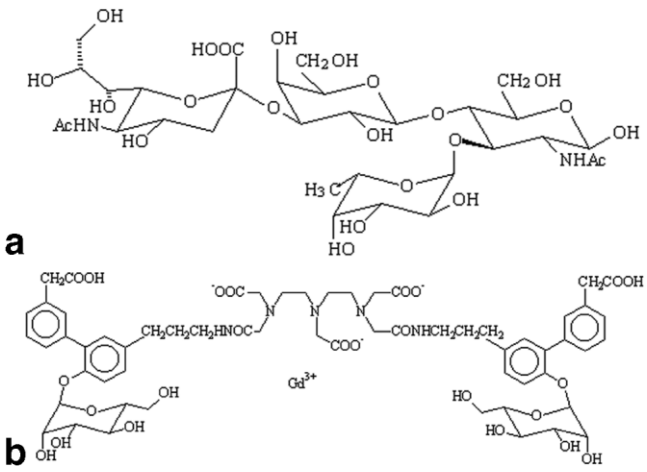

FIG. 1. Molecular structure of sialyl-Lewis^x (**a**) and the E-selectin-targeted contrast agent, Gd-DTPA-B(sLe^x)A (**b**).

group. In previous studies we have shown the synthesis a new contrast agent by grafting the mimetic structure onto a molecule of Gd-DTPA, the parent nonspecific and extracellular contrast agent (17,18).

In the present work, the E-selectin-targeted contrast agent was evaluated in mice and rats with respect to its pharmacokinetics, biodistribution, and potential to image inflammation by MRI. A fulminant hepatitis model was used in which the pathological conditions were induced by the co-administration of D-galactosamine and lipopolysacharide (19,20). The neutrophil adhesion to the sinusoid wall is an early event in this process of liver inflammation, which is related to the E-selectin expression during the first few hours (21). This animal model was chosen for two reasons: 1) in humans, E-selectin is up-regulated on sinusoidal lining cells throughout the liver parenchyma in acute hepatitis (22,23); and 2) a strong, focal expression of E-selectin on hepatic endothelium has been detected in patients with alcoholic hepatitis (24), primary biliary cirrhosis, and acute allograft rejection (25).

MATERIALS AND METHODS

Synthesis of the Contrast Agent

The synthesis of the E-selectin-targeted contrast agent (Gd-DTPA-B(sLe^x)A) was recently described (17). Briefly, a 12-step synthesis scheme with an overall yield of 5% was used to obtain the Gd-DTPA derivative carrying two groups of 3-(2α-D-mannopyranosyloxyphenyl) phenyl acetic acid (Fig. 1).

Relaxometry

The proton longitudinal relaxivity in water and rat blood was measured at 60 MHz and 37°C on a Bruker Minispec mq60 (Bruker, Karlsruhe, Germany).

Enzyme-Linked Immunosorbent Assay (ELISA) Test of Affinity for E-Selectin

We assessed the specific interaction of Gd-DTPA-B(sLe^x)A with E-selectin by means of an ELISA test, using the competition between the contrast agent and the natural ligand of E-selectin, Sialyl Le^x. Recombinant mouse E-selectin/Fc chimera (R&D Systems Europe Ltd., Oxon, UK) was immobilized on protein A-coated ELISA plates (PERBIO Science, Erembodegem-Aalst, Belgium) according to the supplier's instructions. Various concentrations of Gd-DTPA-B(sLe^x)A (300 μM, 30 μM, 0.03 μM) were incubated with 30 μM Sialyl Le^x (Sialyl Le^x-PAA-biotin; GlycoTech Corp., Gaithersburg, MD) in TBS buffer (50 mM Tris-HCl, 150 mM NaCl, 0.02% NaN_3, 1 mM $CaCl_2$, pH 7.4) for 90 min at room temperature. Control samples were prepared to determine the level of Sialyl Le^x-PAA-biotin binding in the absence of Gd-DTPA-B(sLe^x)A. After the samples were washed three times with TBS buffer, they were incubated with peroxidase-conjugated streptavidin (Sigma-Aldrich, Bornem, Belgium) diluted 1:400 in TBS for 1 hr at room temperature. The wells were washed three times with TBS and incubated with 0.2 mL of 22 mg % peroxidase substrate (ABTS (2,2′-azino-bis(3-ethylbenzothiazoline-6sulfonate) diamonium salt); Sigma-Aldrich, Bornem, Belgium) prepared in 50 mM sodium citrate, pH 4.0. The OD_{405} was measured after 30 min of incubation at room temperature. The results represent means of triplicate determinations (±SEM) and were expressed as percentages of Sialyl Le^x-PAA-biotin binding in the presence of Gd-DTPA-B(sLe^x)A related to noninhibited binding (i.e., in the absence of Gd-DTPA-B(sLe^x)A).

Animal Studies

All of the animal experiments met the requirements of the ethics committee of our institution. MRI and biodistribution studies were performed on male Balb/Cby JICo mice (mean weight = 25 ± 5 g; Iffa Credo, Brussels, Belgium). Male Wistar rats (mean weight = 150 ± 25 g; Iffa Credo, Brussels, Belgium) were used to assess the plasma pharmacokinetics of the contrast agent. The animals were anesthetized with 50 mg/kg b.w., i.p. Nembutal (Sanofi, Brussels, Belgium). The contrast agents (Gd-DTPA-B(sLe^x)A, and Gd-DTPA as control) were administered as a bolus via the femoral vein at a dose of 0.1 mmole/kg to healthy animals (controls) and animals with hepatitis.

Experimental Model of Fulminant Hepatitis

D-galactosamine hydrochloride (Sigma-Aldrich, Bornem, Belgium), dissolved in phosphate-buffered saline (PBS), was injected i.p. at a dose of 2 g/kg. *Escherichia coli* 026:B6 lipopolysaccharide (LPS; Sigma-Aldrich, Bornem, Belgium) was administered via the tail vein at a dose of 400 μg/kg after it was dissolved in PBS. The fulminant hepatitis appeared 6 hr after this co-administration of D-galactosamine and LPS (19,20,26).

MRI and Data Analysis

MRI was performed on a Siemens® Magnetom Impact System 1.0 T (40 MHz; CHAMBOR Clinical MRI Center, Mons, Belgium) with the use of a small-FOV surface coil (11-cm diameter). A T_1-weighted spin-echo sequence was used with the following parameters: TR/TE = 600/20 ms; FOV = 5 × 10 cm; matrix = 90 × 256; 6 slices; slice thickness = 3 mm; spatial resolution = 0.555 × 0.390 mm. One precontrast and several postcontrast images were acquired (three animals per experimental group) every 10 min for up to 60 min.

Signal intensity (SI) values for each time delay were measured within several ROIs in the liver and a Gd phantom with an in-house-built image analysis software (27). The liver SI values were normalized with respect to the Gd phantom. The data were averaged and the standard error was calculated for each time point. SI enhancement was defined as the ratio of the difference between pre- and postcontrast SI to precontrast SI.

Plasma Pharmacokinetics

For determination of the plasma pharmacokinetics, male Wistar rats (three animals per experimental group) were tracheotomized, and the left carotid artery was catheterized (Becton Dickinson Angiocath; 0.7 × 19 mm) for blood collection. Blood samples (~0.3 mL) were collected (with intravenous saline replacement) before and at 1, 2.5, 5, 15, 30, 45, 60, 90, and 120 min after the injection of the contrast agent. Since the contrast agent does not bind to proteins (see below), the gadolinium (Gd) content of the blood samples was determined by relaxometry at 37°C and 60 MHz on a Bruker Minispec. A two-compartment distribution model was used to calculate the pharmacokinetic parameters: the distribution and elimination halflives ($T_{d1/2}$, $T_{e1/2}$), the apparent volume of distribution (VD_β), the total clearance (Cl_{tot}), and the initial blood concentration C_0 (28). We converted the Gd concentrations in blood to plasma concentrations by assuming a hematocrit value of 0.53 (blood volume = 58 mL/kg; plasma volume = 31 mL/kg) (29).

Biodistribution

The biodistribution studies were performed on mice (N = 3 for sampling times 10–45 min, N = 10 for the 60-min sampling time) that were killed at different time intervals (10, 30, 45, and 60 min) after the injection of 0.1 mole/kg contrast agent. Samples of the liver, kidneys, and spleen were collected, weighed, dried overnight at 70°C, and subsequently digested (up to 0.4 g each sample) under acidic conditions (3 mL HNO_3, 1 mL H_2O_2) by microwaves (Milestone MSL-1200, Sorisole, Italy). The Gd content was determined by inductively coupled plasma-atomic emission spectroscopy (ICP-AES; Jobin Yvon JY70+, Longjumeau, France). The results are expressed as percentages of the injected dose/g (%ID/g).

RESULTS

Relaxivity of Gd-DTPA-B(sLe^x)A

The relaxivities of 3.46 s^{-1} mM^{-1} and of 4.61 s^{-1} mM^{-1} in aqueous solution and in rat blood were measured at 60 MHz and 37°C, respectively. These values, which are comparable to those observed with Gd-DTPA (3.34 s^{-1} mM^{-1} and 4.35 s^{-1} mM^{-1}), exclude a binding to blood plasma proteins. This fact is important because competing interactions would be unfavorable for the final targeting of E-selectin at the sites of inflammation by Gd-DTPA-B(sLe^x)A, as well as for the dosage by relaxometry.

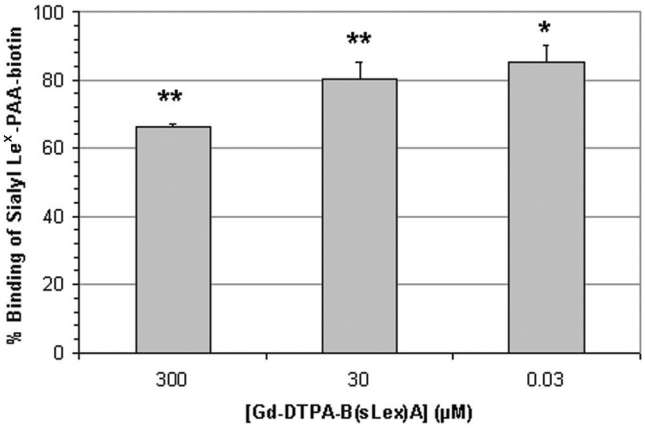

FIG. 2. Competition of Gd-DTPA-B(sLe^x)A (300 μM, 30 μM, 0.03 μM) with 30 μM Sialyl Le^x-PAA-biotin performed in vitro by ELISA. The results represent averages of triplicate determinations (±SEM) and are expressed as percentages of Sialyl Le^x-PAA-biotin binding in the presence of Gd-DTPA-B(sLe^x)A related to noninhibited binding (i.e., in the absence of Gd-DTPA-B(sLe^x)A). Student's t-test was used to calculate Sialyl Le^x-PAA-biotin binding in the presence of Gd-DTPA-B(sLe^x)A vs. noninhibited binding: ** $P < 0.01$, * $P < 0.05$.

Validation of the Specific Interaction of Gd-DTPA-B(sLe^x)A With E-Selectin

The specific interaction of Gd-DTPA-B(sLe^x)A with E-selectin was evaluated by an ELISA test of competition with Sialyl Le^x-PAA-biotin (Fig. 2). The results were expressed as percentages of Sialyl Le^x-PAA-biotin binding (ranges of concentration: 300 μM, 30 μM, and 0.03 μM) to E-selectin in the presence of Gd-DTPA-B(sLe^x)A (30 μM). The results show that Gd-DTPA-B(sLe^x)A inhibited the Sialyl Le^x-PAA-biotin binding to E-selectin by 15–34%, depending on the concentration of the contrast agent. It is evident that Gd-DTPA-B(sLe^x)A preserves a high affinity for this adhesion molecule, since it induced 20% inhibition ($P < 0.01$) of Sialyl Le^x-PAA-biotin binding at equivalent concentrations (30 μM).

MRI Studies of Gd-DTPA-B(sLe^x)A

Figure 3 shows coronal views of a healthy mouse (Fig. 3a) and a mouse with hepatitis (Fig. 3b) obtained before and at several time intervals after i.v. administration of Gd-DTPA-B(sLe^x)A. The images acquired up to 1 hr after administration of the agent show no significant and persistent contrast enhancement in the liver of the healthy mouse. The urinary bladder is apparent and is filled with contrast agent 30 min after its injection, which attests to the excretion of the compound. In the precontrast image of the mouse with hepatitis, the liver blood vessels appear

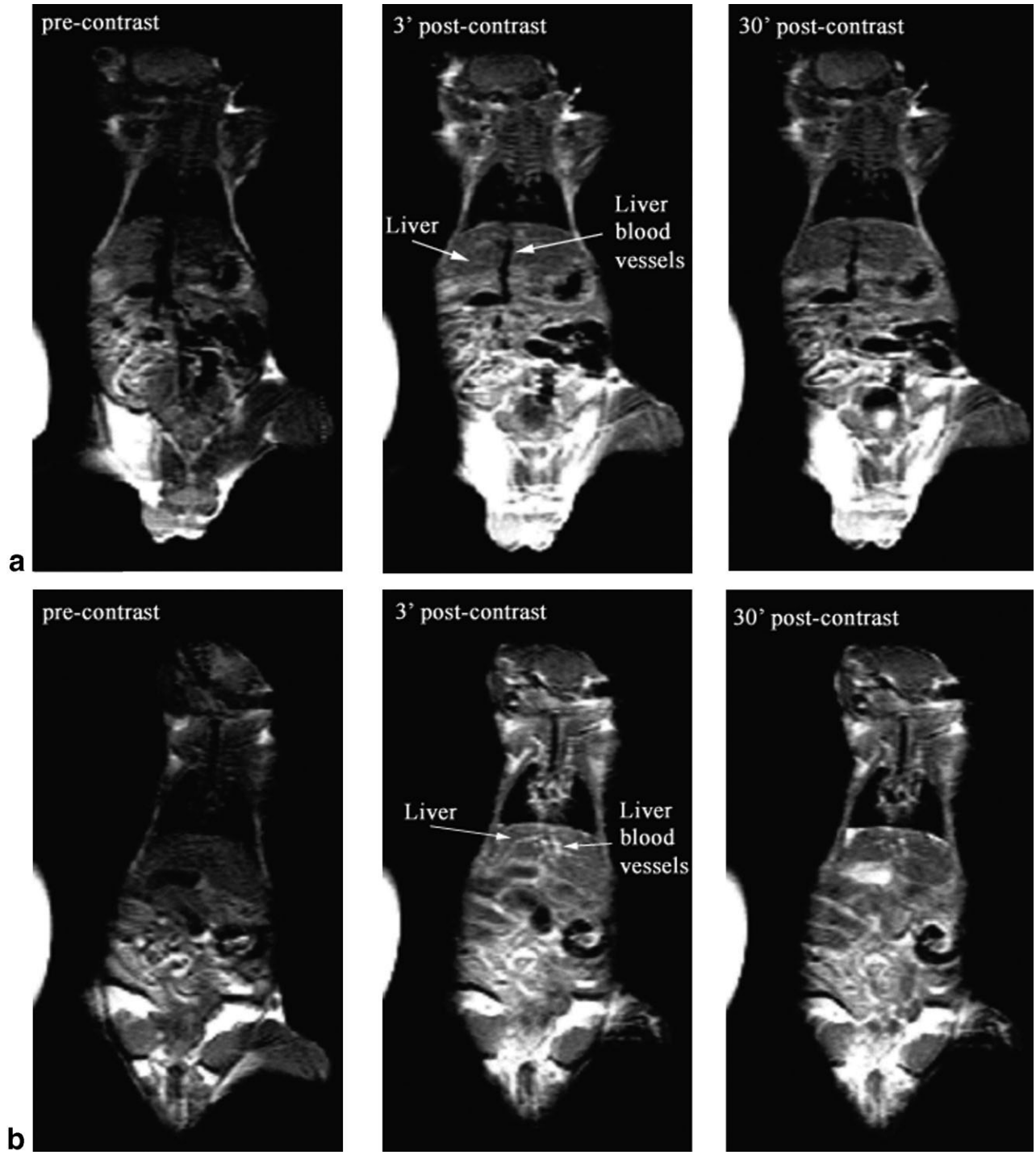

FIG. 3. MR coronal images of a healthy mouse (**a**) and a mouse with hepatitis (**b**) before and several time intervals after i.v. administration of Gd-DTPA-B(sLe^x)A. The images were obtained with a Siemens® Magnetom Impact System at 1.0 T. Note: The urinary bladder of the healthy mouse (**a**) is apparent and is filled with contrast agent 30 min after its injection, which attests to the excretion of the compound.

dark compared to the parenchyma. However, they become bright in the postcontrast images, and the enhancement persists over 60 min. The enhancement of other systemic blood vessels, including the heart, is noticeable in pathological conditions. Gd-DTPA did not produce any contrast between blood vessels and liver parenchyma in healthy mice and mice with hepatitis over the same period (not shown).

The relative change of postcontrast vs. precontrast SI calculated for the liver of different experimental groups is presented on Fig. 4. For the healthy mice injected with Gd-DTPA-B(sLe^x)A, no significant change was observed in the liver. On the other hand, a rapid and sustained enhancement of SI was noticed in the injured livers after injection of Gd-DTPA-B(sLe^x)A. The SI reached a maximum (55%) 3 min postcontrast and remained at about 35% until the end of the imaging period (60 min). The statistical analysis revealed a significant difference compared to the other experimental groups, such as the Gd-DTPA-treated animals.

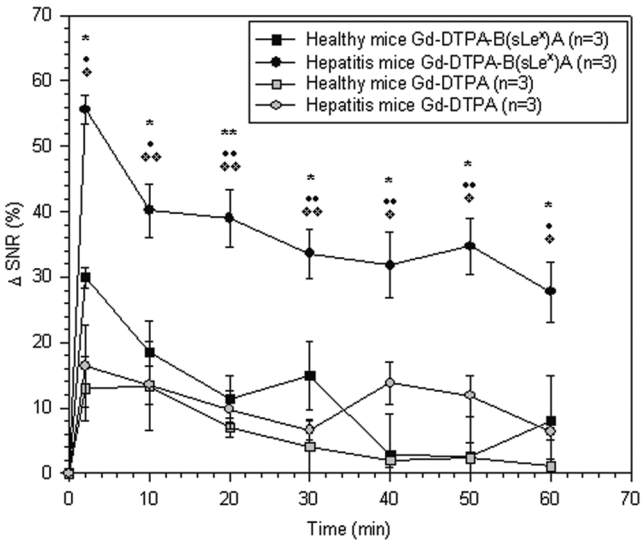

FIG. 4. Percentage change of postcontrast SI vs. time for liver in different experimental groups. The results are represented as averages ± SEM and were statistically processed using Student's *t*-test: ** = $P < 0.01$, * = $P < 0.05$ as compared to healthy mice injected with Gd-DTPA-B(sLe^x)A; ◆◆ = $P < 0.01$ and ◆ = $P < 0.05$ as compared to healthy mice injected with Gd-DTPA; ❖❖ = $P < 0.01$ and ❖ = $P < 0.05$ as compared to mice with hepatitis injected with Gd-DTPA.

Plasma Pharmacokinetics

The pharmacokinetic parameters of Gd-DTPA-B(sLe^x)A were determined for both the healthy rats and those with hepatitis. Gd-DTPA was used as a control. A standard two-compartment model (Fig. 5) can describe the blood pharmacokinetics of both compounds. The data in Fig. 5 are represented as percentages of the plasma concentration C_0 (concentration at time 0) to emphasize the kinetics of blood clearance for each experimental group. We calculated the pharmacokinetic parameters (Table 1) by fitting the curves of blood concentration as a function of time after a single bolus i.v. injection.

The results show a prolonged elimination halflife ($T_{e1/2}$ = 48.9 min in rats with hepatitis; $T_{e1/2}$ = 29.8 min in healthy rats) for Gd-DTPA-B(sLe^x)A, which confirms the MRI data. This pharmacokinetic parameter suggests a slow elimination of Gd-DTPA-B(sLe^x)A that is proved on one hand by the high and sustained contrast enhancement observed in the inflamed liver, and on the other hand by the low and almost unaffected SI in kidneys.

The delayed clearance (2.54 mL/kg/min) in pathological conditions corroborates our previous statements concerning the blood pharmacokinetics. The clearances determined for the other experimental groups are higher and quite similar, which is explained by the nonspecific character of Gd-DTPA and the absence of E-selectin in healthy animals.

The VD_β of Gd-DTPA-B(sLe^x)A ranges between 0.319 L/kg (hepatitis) and 0.311 L/kg (healthy), and is not significantly different from the values observed for Gd-DTPA.

Biodistribution of Gd-DTPA-B(sLe^x)A

The biodistribution of Gd-DTPA-B(sLe^x)A in different organs (e.g., the liver, kidneys, and spleen) up to 1 hr after administration of a single i.v. injection of 0.1 mmol Gd/kg was analyzed in mice under pathological conditions and compared with results from healthy mice and Gd-DTPA (Table 2).

The biodistribution studies confirm the MRI and pharmacokinetic data by demonstrating an elevated liver uptake of Gd-DTPA-B(sLe^x)A in mice with hepatitis (16.22%, $P < 0.01$) as compared to healthy mice (6.72%) early (10 min) after its administration. The same holds true 1 hr after contrast agent administration (12.06% in mice with hepatitis vs. 1.36% in healthy mice).

The route of excretion is probably renal, as suggested by the Gd concentration in the kidneys, which is lower in animals with hepatitis (39.28%) than in healthy ones (64.64%) 10 min after injection.

The Gd concentration of Gd-DTPA-B(sLe^x)A in the spleen is higher during inflammatory pathology (6.50–17.13%) than in the physiological state (2.08–4.71%). The contrast agent may be retained in the spleen because of the interaction with L-selectin expressed by lymphocytes. As previously mentioned, the ligand of L-selectin is also a molecule of the sialyl-Lewis^x type (23).

To confirm the specificity of Gd-DTPA-B(sLe^x)A, we compared its biodistribution with that of Gd-DTPA 1 hr after administration in healthy mice or mice with hepatitis.

Both contrast agents were found in higher concentrations in the liver of animals with hepatitis. However, the level of Gd-DTPA-B(sLe^x)A was superior (12.06%, $P < 0.01$) to that of Gd-DTPA (5.68%), which probably accumulated nonspecifically in the injured liver parenchyma. Nevertheless, the accumulation of Gd-DTPA-B(sLe^x)A in the liver parenchyma is expected to be limited because its

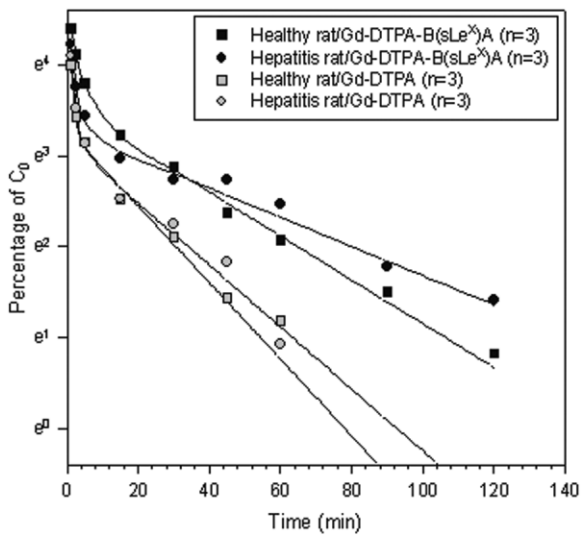

FIG. 5. Blood pharmacokinetic profiles of Gd-DTPA-B(sLe^x)A vs. Gd-DTPA in rats. The data are represented as percentages of C_0. The solid line represents the fit of data to a biexponential profile. For the sake of clarity, the error bars have been excluded.

Table 1
Pharmacokinetic Parameters of Gd-DTPA and Gd-DTPA-B(sLe^x) A Determined in Rats

Pharmacokinetic parameters	Gd-DTPA		Gd-DTPA-B(sLe^x) A	
	Healthy	Hepatitis	Healthy	Hepatitis
$T_{d1/2}$ (min)	0.7 ± 0.04	1.0 ± 0.2	2.1 ± 0.4	1.4 ± 0.2***
$T_{e1/2}$ (min)	14.9 ± 1.2	22.2 ± 1.6	29.8 ± 2.4	48.9 ± 4.8*,***,****
Cl_{tot} (mL/kg/min)	8.66 ± 1.18	7.26 ± 0.69	6.36 ± 0.75	2.54 ± 0.35**,***,****
VD_β (L/kg)	0.205 ± 0.030	0.270 ± 0.042	0.311 ± 0.045	0.319 ± 0.052

The results are represented as averages ± SEM; the Student *t*- test has been calculated for Gd-DTPA-B(sLe^x)A in pathological conditions vs. each of other experimental groups: ** = P$p < 0.01$, * = $P < 0.05$ as compared to healthy mice injected with Gd-DTPA-B(sLe^x)A: *** = $P < 0.01$ as compared to healthy mice injected with Gd-DTPA: **** = $p < 0.01$ as compared to mice with hepatitis injected with Gd- DTPA. $T_{d1/2}$, distribution halflife; $T_{e1/2}$, elimination halflife; Cl_{tot}, total clearance: VD_β, volume of distribution.

ligand is expressed on vascular endothelium. This is confirmed by the MRI studies, which show an enhancement of the liver blood vessels.

The Gd concentration in kidneys was highest in animals with hepatitis injected with Gd-DTPA-B(sLe^x)A, but this value was not significantly different from Gd-DTPA in similar conditions.

The retention of Gd-DTPA-B(sLe^x)A in spleen has the same causes as explained above. However, a nonspecific accumulation was observed in different organs for both contrast agents in pathological conditions, probably as a consequence of the lesions produced by the co-administration of LPS and D-galactosamine.

DISCUSSION AND CONCLUSIONS

E-selectin, which is absent from normal liver tissue, is strongly expressed on sinusoidal lining cells in inflammatory liver diseases. In the present study, E-selectin was targeted by a specific marker for MRI diagnosis. The new contrast agent mimics the sialyl-Lewis^x molecule, which is the main ligand of E-selectin, and is proposed not only for the morphological diagnosis of inflammatory lesions, but also as a functional marker of immune response. Therefore, Gd-DTPA-B(sLe^x)A could be used successfully to monitor immune reactions during a therapeutic procedure.

The competition performed in vitro with Sialyl Le^x, the natural ligand of E-selectin, proved that Gd-DTPA-B(sLe^x)A interacts specifically with this adhesion molecule. The results show that Gd-DTPA-B(sLe^x)A preserves a high affinity for E-selectin by inhibiting the Sialyl Le^x-PAA-biotin binding by 20% at equivalent concentrations (30 μM).

The MRI studies demonstrate that the new compound significantly enhanced (by 55–35%) the liver blood vessels of the animals with hepatitis over a period of 60 min. Previous studies done with Magnevist® in chronic hepatitis (30) showed a patchy enhancement in acute liver inflammation, which was correlated with hepatocellular damage, while the enhancement of linear-shaped areas in advanced hepatitis indicated the presence of fibrosis. The enhanced areas in our images (Fig. 3b) obtained with Gd-DTPA-B(sLe^x)A on hepatitis are not attributable to fibrotic lesions, since our model of inflammation corresponds to an acute pathology. The systemic blood vessels, including those in the heart, are also enhanced by Gd-DTPA-B(sLe^x)A in pathological conditions, which is explained by a systemic LPS induction of E-selectin expression (31).

The MRI data are confirmed by the pharmacokinetic evaluation and the biodistribution data, which reflect a delayed elimination of Gd-DTPA-B(sLe^x)A and an elevated liver uptake in animals with hepatitis. Its interaction with E-selectin or other adhesion molecules containing a

Table 2
Biodistribution of Gd-DTPA-B(sLe^x)A vs. Time in Healthy Mice and Mice With Hepatitis After Single i.v. Administration of 0.1.mmol Gd/kg

Organs	Gd-DTPA(sLe^x)A (% of ID/g)				Gd-DTPA (% of ID/g)
	10 min	30 min	45 min	60 min	60 min
Liver					
Healthy	6.72 ± 0.29	5.57 ± 0.47	4.75 ± 0.54	1.36 ± 0.25****	2.04 ± 0.14
Hepatitis	16.22 ± 1.80**	11.12 ± 1.53**	8.53 ± 1.05**	12.06 ± 1.27**,***	5.68 ± 0.45*
Kidneys					
Healthy	64.64 ± 3.09	58.20 ± 3.70	34.14 ± 5.76	11.39 ± 1.20	15.66 ± 0.82
Hepatitis	39.28 ± 1.31**	34.82 ± 2.34*	31.62 ± 2.51	41.70 ± 2.29**	39.06 ± 2.50**
Spleen					
Healthy	4.71 ± 0.66	2.88 ± 0.10	1.55 ± 0.15	2.08 ± 0.29	1.62 ± 0.05
Hepatitis	17.13 ± 1.10**	9.06 ± 0.85**	9.43 ± 0.70**	6.50 ± 0.48**	7.62 ± 0.66*

The results represent averages ± SEM. $N = 3$ for the sampling times 10–45 min, $N = 10$ for 60 min sampling time. The data were statistically processed using the Student *t*-test: ** = $P < 0.01$ and * = $P < 0.05$ as compared to healthy mice and for Gd-DTPA-B(sLe^x)A vs. Gd-DTPA (*** = $p < 0.01$; **** = $P < 0.05$).

lectin domain is likely to contribute to the delayed blood clearance by slowing down the elimination phase. In pathological conditions, Gd-DTPA-B(sLe^x)A should accumulate more specifically at sites of inflammation through the interaction with E-selectin expressed on blood vessels, a process that will prolong the elimination halflife. The selectins are suitable to work in flow conditions because of their fast association and dissociation constants (32,33), which enable the adhesion of leukocytes to the vascular endothelium. Since the selective contrast agent reproduces the sialyl-Lewis^x molecule, its interaction with E-selectin should therefore be transient, enabling recirculation in the blood stream and subsequent delayed elimination.

An accumulation also observed in other organs (e.g., the liver, kidneys, and spleen) is attributable to the lesions produced by this inflammatory model. Additionally, LPS is known to induce acute renal failure associated with a fall in the glomerular filtration rate and a variable reduction in the renal blood flow (34). This phenomenon may contribute to the delayed blood clearance, combined with a partial nonspecific accumulation in different organs. Still, our data reflect a specific retention of Gd-DTPA-B(sLe^x)A in pathological conditions.

This work thus confirms the potential of Gd-DTPA-B(sLe^x)A, as was recently demonstrated in the context of brain injury and inflammation (35,36).

Gd-DTPA-B(sLe^x)A shows promise as an in vivo tool for the noninvasive analysis of E-selectin expression in inflammatory disorders. This notion is supported by the fact that it provides a significant and prolonged contrast enhancement, a long vascular residence time, and an elevated uptake in inflamed tissue.

ACKNOWLEDGMENTS

The authors thank Mrs. Patricia de Francisco for her help in preparing the manuscript. Dr. Luisa Divano and Mr. Jacques Van Espen from CHAMBOR Clinical MRI Center (Mons, Belgium) are acknowledged for the 1.0 T imaging sessions.

REFERENCES

1. Rennen HJJM, Boerman OC, Oyen WJG, Corstens FHM. Imaging infection/inflammation in the new millennium. Eur J Nucl Med 2001;28: 241–252.
2. Iwamoto I. Drugs and the immune system. In: Page CP, Curtis MJ, Sutter MC, Walker MJA, Hoffman BB, editors. Integrated pharmacology. London, Chicago, Philadelphia, St. Louis, Sydney, Tokyo: Mosby International; 1997. p 319–325.
3. Albelda SM, Buck CA. Integrins and other cell adhesion molecules. FASEB J 1990;4:2868–2880.
4. Smith CW. Endothelial adhesion molecules and their role in inflammation. Can J Physiol Pharmacol 1993;71:76–87.
5. Roitt IM, Brostoff J, Male DK. Immunology. 2nd ed. London, New York: Churchill Livingstone, Gover Medical Publishing; 1990.
6. Nunn AD, Linder KE, Tweedle MF. Can receptors be imaged with MRI agents? Q J Nucl Med 1997;41:155–162.
7. Rovaris M, Filippi M. Contrast enhancement and the acute lesion in multiple sclerosis. Neuroimaging Clin N Am 2000;10:705–717.
8. Park JH, Olsen NJ. Utility of magnetic resonance imaging in the evaluation of patients with inflammatory myopathies. Curr Rheumatol Rep 2001;3:334–345.
9. McGonagle D, Conaghan PG, Wakefield R, Emery P. Imaging the joints in early rheumatoid arthritis. Best Pract Res Clin Rheumatol 2001;15: 91–104.
10. Reynier C, Garcier J, Legault B, Motreff P, Ponsonnaille J, Ravel A, De Riberolles C, Boyer L. Cross-sectional imaging of post endocarditis paravalvular myocardial abscesses of native mitral valves: 4 cases. J Radiol 2001;82:665–669.
11. Kamochi M, Kamochi F, Kim YB, Sawh S, Sanders JM, Sarembock I, Green S, Young JS, Fu SM, Rose CE. P-selectin and ICAM-1 mediate endotoxin-induced neutrophil recruitment and injury to the lung and liver. Am J Physiol Lung Cell Mol Physiol 1999;277:L310–L319.
12. Wyble CW, Hynes KL, Kuchibhotla J, Marcus BC, Hallahan D, Gewertz BL. TNF-alpha and IL-1 upregulate membrane-bound and soluble E-selectin through a common pathway. J Surg Res 1997;73:107–112.
13. Josephs MD, Bahjat FR, Fukuzuka K, Ksontini R, Solorzano CC, Edwards III CK, Tannahill CL, MacKay SLD, Copeland III EM, Moldawer LL. Lipopolysaccharide and D-galactosamine-induced hepatic injury is mediated by TNF-α and not by Fas ligand. Am J Physiol Regul Integr Comp Physiol 2000;278:R1196–R1201.
14. Nowak M, Gaines GC, Rosenberg J, Minter R, Bahjat FR, Rectenwald J, MacKay SLD, Edwards III CK, Moldawer LL. LPS-induced liver injury in D-galactosamine-sensitized mice requires secreted TNF-α and the TNF-p55 receptor. Am J Physiol Regul Integr Comp Physiol 2000;278: R1202–R1209.
15. Kang HW, Josephson L, Petrovsky A, Weissleder R, Bogdanov A. Magnetic resonance imaging of inducible E-selectin expression in human endothelial cell culture. Bioconjugate Chem 2002;13:122–127.
16. Kogan TP, Dupré B, Keller KM, Scott IL, Bui H, Market RV, Beck PJ, Voytus JA, Revelle BM, Scott D. Rational design and synthesis of small molecules, non-oligosaccharide selectin inhibitors: (α-Mannopyranosyloxy)-biphenyl-substituted carboxylic acids. J Med Chem 1995;38: 4976–4984.
17. Fu Y, Laurent S, Muller RN. Synthesis of a Sialyl Lewis X mimetic conjugated with DTPA, potential ligand of new contrast agents for medical imaging. Eur J Org Chem 2002;3966–3973.
18. Laurent S, Vander Elst L, Fu Y, Muller RN. Synthesis and characterization of Gd-DTPA-B(sLe^x)A, a new MRI contrast agent targeted to inflammation. Bioconjugate Chem 2004;15:99–103.
19. Galanos C, Freudenberg MA, Reutter W. Galactosamine-induced sensitization to the lethal effects of endotoxin. Proc Natl Acad Sci USA 1979;76:5939–5943.
20. Camara DS, Caruana JA, Schwartz KA, Montes M, Nolan JP. D-Galactosamine liver injury: absorption of endotoxin and protective effect of small bowel and colon resection in rabbits (41555). Proc Soc Exp Biol Med 1983;172:255–259.
21. Lawson JA, Burns AR, Farhood A, Bajt ML, Collins RG, Smith CW, Jaeschke H. Pathophysiologic importance of E- and P-selectin for neutrophil-induced liver injury during endotoxemia in mice. Hepatology 2000;32:990–998.
22. Volpes R, Van den Oord JJ, Desmet VJ. Vascular adhesion molecules in acute and chronic liver inflammation. Hepatology 1992;15:269–275.
23. Jaeschke H, Smith CW, Clemens MG, Ganey PE, Roth RA. Contemporary issues in toxicology. Mechanisms of inflammatory liver injury: adhesion molecules and cytotoxicity of neutrophils. Toxicol Appl Pharmacol 1996;139:213–226.
24. Adams DH, Burra P, Hubscher SG, Elias E, Newman W. Endothelial activation and circulating vascular adhesion molecules in alcoholic liver disease. Hepatology 1994;19:588–594.
25. Adams DH, Hubscher SG, Fisher NC, Williams A, Robinson M. Expression of E-selectin and E-selectin ligands in human liver inflammation. Hepatology 1996;24:533–538.
26. MacDonald JR, Beckstead JH, Smuckler EA. An ultrastructural and histochemical study of the prominent inflammatory response in D(+)-galactosamine hepatotoxicity. Br J Exp Pathol 1987;68:189–199.
27. Amorison A. Creation of parametric images by fast treatment of dynamic data. Application to the clinical methods of morphologic and functional investigation. Ph.D. dissertation, Polytechnics Faculty of Mons, Mons, Belgium, 1999.
28. Parmelee DJ, Walovitch RC, Ouellet HS, Lauffer RB. Preclinical evaluation of the pharmacokinetics, biodistribution, and elimination of MS-325, a blood pool agent for magnetic resonance imaging. Invest Radiol 1997;32:741–747.

29. Misselwitz B, Schmitt-Willich H, Ebert W, Frenzel T, Weinmann HJ. Pharmacokinetics of gadomer-17, a new dendritic magnetic resonance contrast agent. MAGMA 2001;12:128–134.
30. Semelka RC, Chung J-J, Hussain SM, Marcos H, Woosley JT. Chronic hepatitis, correlation of early patchy and late linear enhancement patterns on gadolinium-enhanced MR images with histopathology initial experience. J Magn Reson Imaging 2001;13:385–391.
31. Kadl A, Huber J, Gruber F, Bochkov VN, Binder BR, Leitinger N. Analysis of inflammatory gene induction by oxidized phospholipids in vivo by quantitative real-time RT-PCR in comparison with effects of LPS. Vascul Pharmacol 2002;38:219–227.
32. Jacob GS, Kirmaier C, Abbas SZ, Howard SC, Steininger CN, Welply JK, Scudder P. Binding of sialyl Lewis X to E-selectin as measured by fluorescence polarization. Biochemistry 1995;34:1210–1217.
33. Levin JD, Ting-Beall HP, Hochmuth RM. Correlating the kinetics of cytokine-induced E-selectin adhesion and expression on endothelial cells. Biophys J 2001;80:656–667.
34. Schwartz D, Brasowski E, Raskin Y, Schwartz IF, Wolman Y, Blum M, Blantz RC, Iaina A. The outcome of non-selective vs selective nitric oxide synthase inhibition in lipopolysaccharide treated rats. J Nephrol 2001;14:110–114.
35. Sibson NR, Blamire AM, Bernades-Silva M, Laurent S, Boutry S, Muller RN, Styles P, Anthony DC. MRI detection of early endothelial activation in CNS inflammation. Magn Reson Med 2004;51:248–252.
36. Barber PA, Foniok T, Kirk D, Buchan AM, Laurent S, Boutry S, Muller RN, Hoyte L, Tomanek B, Tuor UI. MR molecular imaging of early endothelial activation in focal ischemia. Ann Neurol 2004;56: 116–120.